Gupta *et al.*
Future Journal of Pharmaceutical Sciences (2024) 10:19
https://doi.org/10.1186/s43094-024-00581-w

Future Journal of Pharmaceutical Sciences

RESEARCH

Open Access

Preparation and in vitro evaluation of BBG-250 loaded liposomal formulation for anticancer potential

Twinkle Gupta[1], Priyanshu Nema[1], Sakshi Soni[1], Vivek Yadav[2], Sanyog Jain[2], Vandana Soni[1] and Sushil K. Kashaw[1*]

Abstract

Background Liposome-mediated drug delivery systems have emerged as a promising avenue for enhancing cancer treatment strategies. This study aims to develop and assess liposomal carriers loaded with Brilliant Blue G-250 (BBG-250), a potent P2X7 receptor antagonist that shows potential as an anti-tumor agent. Specifically, two types of liposomal formulations were designed: conventional liposomes composed of hydrogenated soya phosphatidylcholine (HSPC) and cholesterol, and pH-sensitive liposomes consisting of dioleoylphosphatidylethanolamine (DOPE), distearoylphosphatidylethanolamine-methoxy polyethylene glycol (DSPE-mPEG), dipalmitoylphosphatidylcholine (DPPC), and cholesterol. The investigation focuses on understanding the morphological characteristics, size, stability, drug incorporation efficiency, drug release profiles, blood compatibility, and cytotoxicity of these liposomal formulations.

Results Advanced photon correlation spectroscopy using the Nano Plus-3 instrument was employed to evaluate the liposomes. The optimized conventional liposomes (HSPC-cholesterol ratio 7:3) exhibited a size of 125 ± 0.3 nm with a polydispersity index (PDI) of 0.21, indicating uniformity. The pH-sensitive liposomes (DOPE:DPPC:DSPE-PEG2000: Cholesterol 4:3:3:0.3) demonstrated a size of 118 ± 1.2 nm with a PDI of 0.230. Zeta potential measurements confirmed the stability of both formulations under physiological conditions, with values of − 16.93 mV for conventional liposomes and − 25.21 mV for pH-sensitive liposomes. Higher drug-to-lipid ratios were found to enhance drug incorporation efficiency. pH-sensitive liposomes exhibited superior drug release characteristics, with 95% release over 24 h, compared to conventional liposomes, which released 70% of the drug. Blood compatibility assessments revealed the safety of both formulations for intravenous administration. Cytotoxicity studies conducted on A549 cell lines demonstrated the cytocompatibility of both liposomal types across a range of concentrations, with IC_{50} values surpassing those of the reference drug, docetaxel.

Conclusions This study underscores the potential of liposomal carriers as effective vehicles for delivering BBG-250, highlighting their stability, biocompatibility, and controlled drug release properties. Despite being slightly less potent than the reference drug, docetaxel, these liposomal formulations hold promise for advancing anticancer strategies. The findings contribute to the evolving landscape of innovative cancer therapy drug delivery systems, offering a novel approach to improving treatment outcomes for cancer patients. The successful development and evaluation of these liposomal carriers pave the way for further investigations and potential clinical applications in the field of cancer therapeutics.

*Correspondence:
Sushil K. Kashaw
sushilkashaw@gmail.com
Full list of author information is available at the end of the article

Springer Open

© The Author(s) 2024. **Open Access** This article is licensed under a Creative Commons Attribution 4.0 International License, which permits use, sharing, adaptation, distribution and reproduction in any medium or format, as long as you give appropriate credit to the original author(s) and the source, provide a link to the Creative Commons licence, and indicate if changes were made. The images or other third party material in this article are included in the article's Creative Commons licence, unless indicated otherwise in a credit line to the material. If material is not included in the article's Creative Commons licence and your intended use is not permitted by statutory regulation or exceeds the permitted use, you will need to obtain permission directly from the copyright holder. To view a copy of this licence, visit http://creativecommons.org/licenses/by/4.0/.

Keywords Allosteric binding, Liposomal formulation, BBG-250, Blood compatibility, P2X7 receptor

Background

Cancer, a complex and multifaceted group of diseases characterized by uncontrolled cell growth and division, continues to be a major global health challenge. It is responsible for an enormous burden of suffering and mortality, with nearly 10 million deaths attributed to cancer in 2020 alone. The intricate interplay of genetic, environmental, and lifestyle factors contributes to the initiation and progression of cancer, rendering it a formidable adversary that requires innovative and targeted therapeutic approaches. In the realm of cancer, lung cancer occupies a particularly sinister position. It stands as one of the most prevalent and lethal forms of malignancy, causing an alarming number of deaths annually. In 2020, lung cancer accounted for a staggering 1.80 million fatalities, thereby solidifying its grim distinction as the leading cause of cancer-related death worldwide. The statistics paint a stark picture of the devastating impact of this disease on individuals, families, and societies at large (ACS, 2020, 2022, 2023). Among the spectrum of lung cancers, non-small cell lung cancer (NSCLC) emerges as the dominant subtype, encompassing a majority of cases. The etiology of NSCLC is intricately linked to diverse factors, including smoking, exposure to environmental pollutants, genetic predisposition, and aging. Its insidious nature often results in diagnosis at advanced stages, significantly hampering treatment success and patient prognosis. Central to addressing the challenge of lung cancer is an understanding of the critical role that cancer stages play in shaping outcomes. Stage of cancer refers to the extent to which it has progressed within the body, ranging from localized disease confined to its site of origin to invasive cancer that has spread to distant regions. This staging system provides valuable insights into the potential for disease eradication, recurrence, and overall survival. In the context of lung cancer, early detection and treatment significantly improve patient outcomes. Unfortunately, a substantial proportion of cases are diagnosed at later stages, severely limiting therapeutic interventions.

Traditional treatments for lung cancer, including surgery, radiation therapy, and chemotherapy, have made strides in extending survival and improving the quality of life[1]. However, the pursuit of more effective and targeted therapeutic strategies remains paramount. The advent of molecular and genetic insights into cancer biology has unveiled novel opportunities for precision medicine. Targeted therapies, immunotherapies, and combination regimens are reshaping the landscape of lung cancer treatment, offering hope for improved outcomes and personalized care [2, 3]. One intriguing avenue of research in the pursuit of innovative lung cancer therapies is the exploration of purinergic receptors, specifically P2X and P2Y subfamilies[4, 5]. These receptors, widely distributed throughout the body, are pivotal players in cellular signaling and communication. Of particular interest is the P2X7 receptor, which exhibits distinct expression patterns in both normal and cancerous lung cells. This receptor not only influences cell proliferation but also plays a crucial role in the delicate balance between cell survival and apoptosis, a programmed cell death mechanism. Importantly, in the context of lung cancer, alterations in P2X7 receptor activity have been implicated in disease progression. The intriguing interplay between the P2X7 receptor and lung cancer opens up an avenue for therapeutic intervention [6]. One compound of interest in this context is Brilliant Blue G-250 (BBG-250), a known antagonist of the P2X7 receptor [7]. Previous studies have demonstrated its ability to modulate receptor activity and impact cellular responses. Harnessing the potential of BBG-250 as a targeted therapy could pave the way for a more nuanced and effective approach to tackling lung cancer. To enhance the precision and efficacy of therapeutic interventions, nanotechnology has emerged as a transformative tool. Liposomes, with their minuscule dimensions and unique physicochemical properties, offer a platform for targeted drug delivery and controlled release. The concept of encapsulating therapeutic agents within nanocarriers holds the promise of minimizing systemic toxicity, maximizing drug accumulation at tumor sites, and ultimately improving treatment outcomes [8]. Liposomes, a well-established type of nanovesicle, have garnered considerable attention in drug delivery applications. Comprising a lipid bilayer surrounding an aqueous core, liposomes offer versatility in encapsulating a wide range of molecules, including hydrophilic and hydrophobic drugs [9]. Their potential to traverse biological barriers, selectively accumulate in tumor tissues, and release their cargo in a controlled manner has spurred interest in their use for cancer therapy. The present research endeavors to explore the computational screening approaches, such as homology modeling molecular docking and ADMET analysis, which were used to evaluate binding affinity between the target (P2X7) and Ligand (BBG-250). The potential interaction of BBG-250 with crucial amino acid residues within target binding pockets has been a subject of investigation in this study. Afterward,

pharmacokinetic parameters were checked via an in silico ADMET study. Then after the potential of liposomal formulations encapsulating BBG-250 for targeted therapy in lung cancer. The overarching objective is to harness the unique attributes of liposomes to enhance the delivery and efficacy of BBG-250 while minimizing adverse effects[10]. By delving into the formulation, characterization, and performance of these liposomal carriers, this study seeks to contribute to the growing body of knowledge aimed at advancing precision medicine strategies for lung cancer treatment. The subsequent sections of this research paper delve into the intricate details of this investigation, encompassing the methodology, results, and discussions that underpin the pursuit of innovative and effective lung cancer therapeutics. Through meticulous analysis and comprehensive assessment, this research endeavors to shed light on the potential of liposomal BBG-250 as a promising avenue for enhancing lung cancer treatment outcomes[11, 12].

Material

The selection and procurement of materials form the foundation of any scientific investigation. Each component contributes to the precision and reliability of experimental outcomes. The following section outlines the various materials employed in this study, including their sources and roles in the research process.

In silico study

Homology modeling

Comparative or homology protein modeling is a powerful 3D protein modeling tool that can predict the conformation of experimentally unavailable protein structure that has amino acid sequences similar to template protein sequence due to the unavailability of P2X7 receptor 3D structure in the PDB. It is difficult and time-consuming to establish the 3D structure of a P2X7 protein using experimental techniques including NMR, X-ray crystallography, and cryo-electron microscopy. Therefore, P2X7 protein structure determination is crucial for planning and evaluating biological research in this scenario. Homology modeling has proven to be the most effective method for building a reliable 3D model of a P2X7 protein from its amino acid sequence. The Ramachandran plot, Errat score, and other validation metrics are indicators of the quality of the protein structural geometry. The following list of tools was used for homology modeling:

Homology modeling by different tools

Homology modeling by MODELLER 10.2 module To create constraints on atomic distances, dihedral angles, and other parameters, MODELLER employs the query structures. These constraints are then paired with statistical distributions determined from several homologous structure pairings in the PDB. Sequences and structures are combined by MODELLER to create a comprehensive alignment that may be manually altered and inspected with molecular graphics software. There are five consecutive steps to comparative modeling using the MODELLER 10.2 module. The very first step of modeling involves searching for the 3D structure of proteins related to the target. For this, we have used the site (www.ncbi.nlm.nih.gov) and downloaded the P2X7 receptor sequence in FASTA file format. The second step denotes the selection of templates for alignment with the target. Here, we run BLAST for getting similar sequences and selected ten sequences (PDB_ID:3H9V,4DW0,4DW1,5FLC,5SVH,5SVJ,5U11,5XW6,5YVE,6AH4) as templates based on maximum identity related to the P2X7 protein sequence from a list of generated sequences in Table 1. Out of a total of ten PDB structures, PDB ID_5SVH was found to be more perfect than others. The third step involves aligning the target protein with the template (PDB_5SVH). The fourth step is the model-building step which automatically calculates the 3D model of the target using an auto model class of the module. In this step, a total of 20 homology models have been generated with different conformations. The fifth step is the evaluation step, in this the models were evaluated using the Ramachandran plot and Errat score as Table 2. Again, out of 20 homology models after evaluation model number 10 (**qsec.B99990010.pdb**) was found to be a more accurate model than others[13]**.**

Homology modeling by SwissModel module SwissModel is a web server that accepts a sequence and delivers the model via email. It follows standard protocols for homologue identification, sequence alignment, core backbone determination, and modeling loops and side chains. SwissModel searches a protein database using

Table 1 Templates with the highest degree of similarity to the P2X7 protein sequence

S. No	PDB hits	Identity (%)	Resolution
1	3h9v	88	–
2	4dw0	88	–
3	4dw1	88	–
4	5f1c	86	–
5	5svh	89	2.0
6	5svj	89	2.9
7	5u1l	89	3.4
8	5xw6	86	–
9	5yve	89	3.4
10	6ah4	89	3.3

Table 2 List of Generated Model and their evaluation

Model	Errat	Pro-check	Model	Errat	Pro-check
qseq.B99990001.pdb	4.27	84.4	qseq.B99990011.pdb	14.23	83.5
qseq.B99990002.pdb	10.04	84.7	qseq.B99990012.pdb	8.56	85.9
qseq.B99990003.pdb	3.21	84.1	qseq.B99990013.pdb	16.23	84.7
qseq.B99990004.pdb	13.27	85.6	qseq.B99990014.pdb	17.22	84.4
qseq.B99990005.pdb	11.55	85.9	qseq.B99990015.pdb	15.41	85.6
qseq.B99990006.pdb	14.71	83.8	qseq.B99990016.pdb	16.81	85.3
qseq.B99990007.pdb	6.84	84.4	qseq.B99990017.pdb	12.17	83.2
qseq.B99990008.pdb	17.7	83.5	qseq.B99990018.pdb	18.22	85.3
qseq.B99990009.pdb	7.35	84.7	qseq.B99990019.pdb	7.37	82.4
qseq.B99990010.pdb	**17.27**	**87.1**	qseq.B99990020.pdb	9.54	81.8

Table 3 Templates with the highest degree of similarity to the P2X7 protein sequence

S. No	PDB hits	Identity (%)	Resolution
1	3h9v	88	–
2	4dw0	88	–
3	4dw1	88	–
4	5f1c	86	–
5	5svh	89	2.0
6	5svj	89	2.9
7	5u1l	89	3.4
8	5xw6	86	–
9	5yve	89	3.4
10	6ah4	89	3.3

Table 4 List of generated model

Generated model	Pro-check (%)	Errat
Model 1	87.3	85.47
Model 2	90.8	80.06
Model 3	92.1	76.65
Model 4	93.1	90.79

Table 5 List of generated models and their Validation of I-Tasser server

Generated model	Ramachandran Plot (%)	Errat
Model 1	74.5	88.81
Model 2	74.1	84.32
Model 3	53.0	69.96
Model 4	**75.9**	**89.84**
Model 5	46.4	70.37

Bold value indicates the best model

BLAST and attempts to build a model for any PDB hits. In comparative modeling, a 3D protein model of a P2X7 receptor sequence is generated by extrapolating experimental information from an evolutionary-related protein structure that serves as a template. In SwissModel, the default modeling workflow consists of the following main steps: (1) **Input data:** The target protein amino acid sequence in FASTA format as a plain text from the NCBI database. (2). **Template search:** Data provided in step 1 serve as a query to search for evolutionary-related protein structures against the SWISSMODEL template library SMTL that is 6u9v, 6u9w, 5u2h, and 5u1u. (3) **Template selection:** Templates are ranked according to GMQE and **6u9v** were used for further model building as shown in Table 3. (4). **Model building**: Selected template(6u9v), a four-3D protein model (Table 4) is automatically generated by first transferring conserved atom coordinates as defined by the target template alignment. (5) **Model quality estimation**: To quantify modeling errors and give estimates on expected model accuracy the Ramachandran plot and Errat score provide estimates of the expected quality of the resulting model at the tertiary and quaternary structure level[14].

Homology modeling by I-tasser module A homology model, based on the Amino acid sequence (NCBI database) of the Homo sapience, corresponding to the P2X7 receptor obtained using the I-TASSER server, and five different models were generated as mentioned in Table 5. The confidence of each comparative model obtained by I-TASSER is quantitatively measured by the C-score which is typically in the range of [−5 to 2]. The best-identified 3D model (out of five comparative models) obtained a C-score value of −2.52. The quality of the raw homology model was assessed by the Pro-check server[15, 16].

Our criteria for model selection were stringent, with a significant emphasis on accuracy as reflected in the

Ramachandran favored regions. Following this thorough validation process, Model.4 emerged as the most optimal choice for subsequent docking studies. A detailed account of the validation parameters, encompassing factors such as Ramachandran favored outcomes, is thoroughly documented and presented in Table 7. This transparent documentation underscores the robustness of our model selection process, establishing a solid foundation for the reliability of the chosen receptor model in our study.

Molecular docking

Molecular docking studies of Brilliant Blue G250 dye (Fig. 1) were performed with receptor protein designed by homology modeling method by using Glide module software (Schrodinger Maestro v13.1). The protein was further processed through 'protein preparation wizard' (Maestro wizard v13.1). The generating states and refinement step were used for improving the protein structure including optimization of H-bonded groups, dehydration, and restrained minimization by using default force field OPLS_3. The minimized protein structure was used for the generation of a grid around ligand molecules. Molecular docking studies were performed by the Glide module of Schrodinger Maestro v13.1 on Brilliant Blue G250 Dye. The protein structure was obtained from the homology modeling by SwissModel (Fig. 1C) which passed various evolution tests (Fig. 1A and B) and was pre-processed by using protein preparation wizard in Maestro v13.1. Generating states and refinement step automatically added hydrogen atoms and some essential bonds at the missing sites of the protein molecule. The refinement step has several functions like optimization of hydrogen-bonded groups, removal of water, and restrained minimization using the default force field OPLS_3. After the optimization process, receptor grid generation was processed to locate the binding pocket in the receptor and in the last ligand docking was performed. The activity of the dye (Ligand) depends on the possible interactions of the ligand with various amino acid residues of the targeted protein (P2X7 receptor) as shown in Fig. 2 [17, 18].

Validation of docking results The docking analysis of BBG250 revealed a notable docking score of -9.597. This outcome suggests a high affinity and favorable binding interaction of BBG250 within the target site. Importantly, these results indicate superior activity levels when compared to the reference compound (Docking score: − 4.621), docetaxel, a well-established agent in previous anticancer studies (refer to Table 7). And also validated by the both positive controls (standard inhibitors) and negative controls (known non-inhibitors) within our docking analysis. BBG250 displayed a higher binding affinity when compared to the positive control and nega-

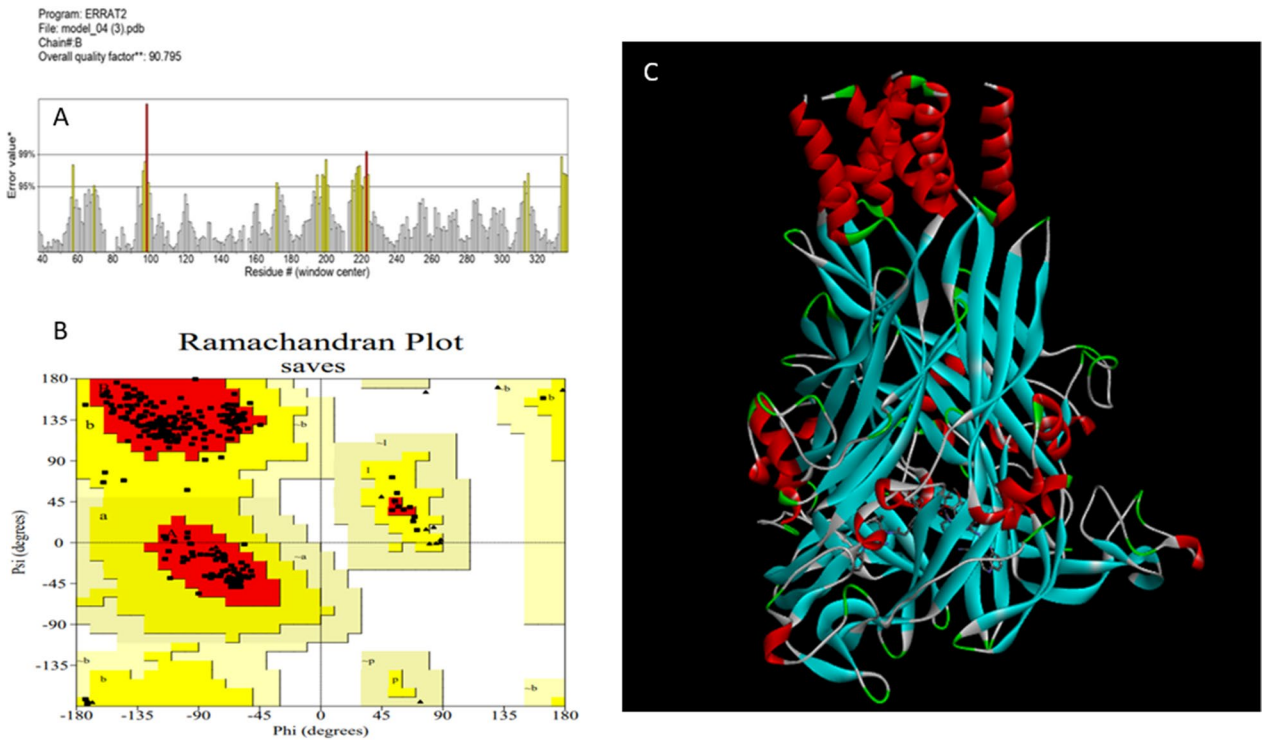

Fig. 1 Representation of **A** Errat score **B** Ramachandran Plot and **C** Generated Best Model

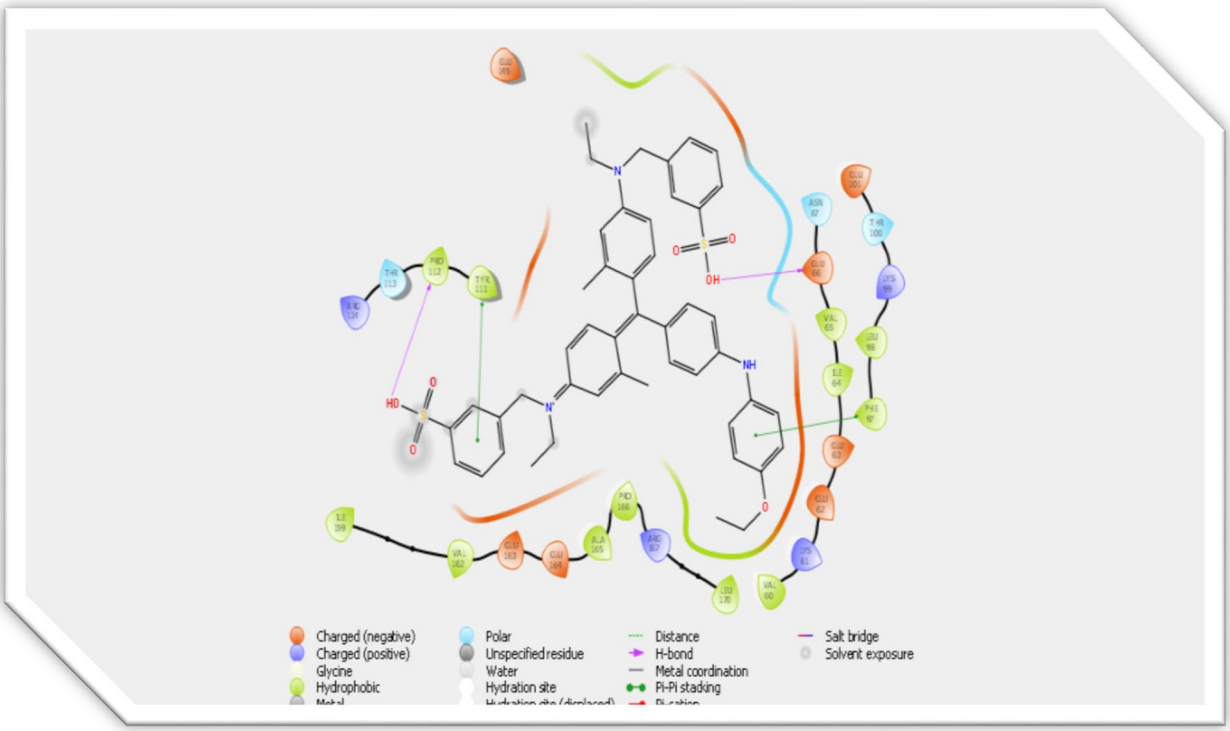

Fig. 2 Representation of Docking Interaction Between P2X7 Homology Model and BBG-250

tive control compounds. This outcome strongly suggests that BBG250 may indeed exhibit superior activity levels compared to previously reported compounds (Table 7). Our research findings substantiate the enhanced potential of BBG250 as a promising candidate in the context of anticancer therapeutics.

Prediction of ADME properties

Nowadays, several online tools and offline software programs are available which help us in predicting the ADME behavior of the drug candidate. In this study, the SwissADME prediction tool (http://www.swissadme.ch/) was used. The compound selected for the ADME study was BBG-250. The compounds were then converted into their canonical 'SMILE' format and put in the 'SwissADME' in the section mentioned as 'Enter a list of SMILES here.' The server predicts the physicochemical properties, lipophilicity, water solubility, pharmacokinetics, druglikeness, lead likeness, and synthetic accessibility of the compounds.

Brilliant blue G-250

The key pharmaceutical agent under scrutiny is BBG-250, a potent antagonist of the P2X7 receptor[10]. This compound, which holds promise for targeted lung cancer therapy, was procured from HIMIDIA Laboratories Ltd, Mumbai, India. Its specialized properties make it an indispensable element in the formulation and subsequent evaluations of liposomal carriers.

Lipids

Lipids are fundamental components of liposomal formulations, providing the structural basis for these liposomes. The lipids used in this study were acquired from distinct sources, each contributing unique attributes to the formulation. mPEG-DSPE, a critical ingredient, was generously provided as a gift sample from Lipoid Germany. This lipid, known for its amphiphilic nature, facilitates the formation of stable liposomes and influences their surface properties. HSPC (hydrogenated soya phosphatidylcholine), a lipid renowned for its biocompatibility and stability, was also a gift sample from Lipoid Germany. Its inclusion in the formulations contributes to the structural integrity of liposomes, enabling efficient encapsulation of BBG-250. DOPE (dioleoylphosphatidylethanolamine), another vital lipid component, was likewise obtained as a gift sample from Lipoid Germany. DOPE presence imparts fluidity and flexibility to the lipid bilayer, optimizing the liposome's ability to encapsulate and release therapeutic agents [19].

Cholesterol

Cholesterol sourced from HiMedia, Mumbai, is a quintessential component of the lipid bilayer. Its role in maintaining membrane integrity, modulating fluidity, and enhancing the stability of liposomal carriers is indispensable [20]. The inclusion of cholesterol in the formulations contributes to the structural integrity and performance of liposomes.

Solvents and filters

Chloroform and methanol, vital solvents in the formulation process, were procured from Department. These solvents play a pivotal role in dissolving lipids and facilitating the formation of thin lipid films, which serve as the foundation for liposomal encapsulation. To ensure the purity and clarity of the formulations, filtration steps were implemented. Nylon filters (AXIVA syringe filters) were employed for this purpose, effectively removing particulate matter and ensuring the quality of liposomal suspensions [21].

Dialysis membrane

For the evaluation of drug release profiles, dialysis membranes are indispensable tools. The dialysis membrane used in this study, sourced from Sigma-Aldrich, boasts a 14 kDa molecular weight cutoff. This semi-permeable barrier allows for controlled diffusion of molecules, facilitating accurate measurement of drug release from liposomal formulations.

The research demanded a range of other chemicals, each contributing to various aspects of the experimental process. These chemicals, all of the highest commercial grade, played roles in diverse procedures, from pH determination to characterization analysis. Their quality and consistency ensured the reliability of the research outcomes. The selection and procurement of materials underpin the scientific rigor and validity of this investigation. Each component, from the therapeutic agent BBG-250 to the lipids, solvents, filters, and membranes, plays a crucial role in formulating, characterizing, and evaluating liposomal carriers for targeted lung cancer therapy.

Preparation of conventional and pH-sensitive liposomes formulation

In the realm of targeted drug delivery, formulation and development of liposomal carriers play a pivotal role in enhancing therapeutic efficacy. This study undertook a systematic approach to engineer liposomal formulations tailored for the encapsulation of BBG-250, a potent P2X7 receptor antagonist with promising implications for lung cancer therapy. Two distinct formulations were meticulously crafted: conventional liposomes composed of hydrogenated soya phosphatidylcholine (HSPC) and cholesterol, and pH-sensitive liposomes consisting of dioleoylphosphatidylethanolamine (DOPE), dipalmitoylphosphatidylcholine (DPPC), DSPE-PEG 2000, and cholesterol [22]. The formulation process, a critical juncture in this research, was executed with precision and methodological rigor.

For the preparation of conventional liposomes, the thin-layer evaporation method was adopted, renowned for its capacity to generate liposomal structures with reproducibility. The process began with the precise weighing of HSPC and cholesterol in a 7:3 ratio ensuring the optimal composition. This lipid mixture was dissolved in a chloroform–methanol solution at a 9:1 ratio, creating an organic phase conducive to liposomal encapsulation [23]. The therapeutic agent BBG-250 was judiciously introduced into the organic phase and fortified with 3.5 mg of the compound to confer the desired therapeutic payload. After solvent evaporation under vacuum at a controlled temperature of 50 °C, a thin lipid film emerged. Hydration of the lipid film with the phosphate-buffered solution (PBS) at pH 7.4 revitalized the structure, forming a homogenous liposomal suspension through Rota evaporation at 50–55 °C and 200 rpm for one hour [24]. Further refinement involved probe sonication for uniformity and size optimization, followed by passage through Sephadex (G-50) column to attain the final liposomal formulation characterized by low polydispersity and targeted size distribution. The resulting liposomes, thus formed, were stored at a controlled 4 °C for subsequent stages of experimentation.

This comprehensive approach to crafting conventional liposomes ensured the creation of structurally sound carriers poised for targeted drug delivery. The subsequent segment will delve into the formulation of pH-sensitive liposomes, shedding light on their unique composition and the intricacies of their preparation.

Characterization of liposomes

FTIR analysis

FTIR (Fourier-transform infrared) analysis was performed to gain insights into the molecular interactions and structural changes present in the formulated liposomes and the Brilliant Blue G-250 (BBG-250) dye. The FTIR spectra of the HSPC liposomes (P11), pH-sensitive formulation (P5), and Brilliant Blue G-250 (BBG-250) were obtained using a Fourier-transform infrared spectrometer. The samples were prepared by depositing a thin film of each formulation on a suitable substrate, followed by scanning within the infrared range. The spectral data obtained were then analyzed to identify specific functional groups and molecular vibrations.

Vesicle shape, size, size distribution, and zeta potential

Vesicle characteristics play a pivotal role in determining the efficacy and behavior of liposomal formulations. Through the utilization of advanced analytical tools, the vesicle size (z-average), size distribution (polydispersity index), and zeta potential (ZP) were meticulously assessed. Using the Nano Plus-3 instrument, the formulations underwent thorough examination employing photon correlation spectroscopy (PCS). Before analysis, the formulations underwent meticulous filtration through a 0.25-micron syringe filter (1:9 v/v) to ensure accuracy. The resulting data were presented thoughtfully, offering a visual representation of these critical parameters [25].

Morphology and structure determination

A profound understanding of the morphology and structural characteristics of liposome preparations was sought through diverse microscopy techniques. Transmission electron microscopy (TEM) was employed to capture distinct features. Glass-mounted HSPC and pH-sensitive liposomes were meticulously examined under phase contrast microscopy, allowing detailed observations at optimal magnification. These observations were thoughtfully documented through photomicrographs, unveiling the distinctive visual attributes of each formulation. Furthermore, a comprehensive TEM study was conducted, involving the creation of thin films on carbon-coated copper grids. These grids, housing the liposome films, were meticulously air-dried and subjected to TEM analysis, providing valuable insights into their internal architecture at magnifications enabled by an accelerating voltage of 200 kV. The resulting images offered a deeper understanding of the structural organization of liposomes [26].

pH determination

The inherent pH values of both types of liposomal formulations were critically assessed, serving as a vital indicator of their stability and compatibility. Measurements were carried out using a precise Elico pH meter, maintaining a controlled temperature of 25 °C ± 0.5 °C. Ensuring the robustness of the findings, the pH determination was conducted in triplicate, reinforcing the accuracy and reliability of the obtained results [27].

Percentage entrapment efficiency

The encapsulation efficiency of the liposomal formulations was quantitatively determined to offer insights into their drug incorporation capabilities. Employing a meticulously designed protocol, liposome pellets underwent dissolution in PBS with 3% Triton X-100, followed by sonication and ultracentrifugation. The resultant process enabled the quantification of percentage entrapment efficiency (%EE). The centrifugation steps, conducted under precise conditions, contributed to accurating measurements. The derived values of %EE were calculated employing established formulas (Eq. 1), providing a quantitative assessment of the formulations' drug incorporation efficacy[28].

$$\%EE = \frac{Weight\ of\ initial\ drug - Weight\ of\ free\ drug}{Weight\ of\ initial\ drug} \times 100 \quad (1)$$

In vitro drug release study

The in vitro drug release profiles of the formulations were meticulously examined, employing a well-established dialysis bag method. In this procedure, the formulations were introduced into dialysis bags, which were immersed in a controlled environment consisting of PBS with a pH of 6.4. Maintained under conditions of controlled temperature (37 °C ± 0.5 °C) and gentle stirring, the formulations' drug release was monitored over 24 h. At regular intervals, samples were withdrawn, and their drug release was quantified through UV spectroscopy. The cumulative drug release data provided valuable insights into controlled release kinetics of the liposomal carriers [29].

Blood compatibility analysis

Evaluating the formulations' compatibility with blood coagulation mechanisms, the PT (prothrombin time) and APTT (activated partial thromboplastin time) assays were deployed. Fresh blood samples, collected in ACD-containing tubes, underwent centrifugation to obtain platelet-poor plasma (PPP). This plasma was subsequently mixed with samples from the formulations, and after an incubation period, PT and APTT were assessed through coagulation analyzer reagent kits. The meticulous evaluation of coagulation parameters allowed for a comprehensive understanding of the formulations' impact on blood coagulation mechanisms, thereby ensuring their biocompatibility [30].

MTT assay: cell viability assessment

The cytotoxic potential of the optimized HSPC and pH-sensitive liposomes was evaluated through MTT [3-(4, 5-dimethylthiazol-2-yl)-2, 5-diphenyl tetrazolium bromide] assay, a widely accepted method for gaging cell viability. Employing A549 cell lines as a model, cells were cultured in 96-well tissue culture plate with cell density of 104 cells/well and were allowed to adhere for 24 h. Following the cell adhesion, cell media was replaced with fresh media containing the treatment sample (2.5, 5, 10, 20, 40, 80 µg/mL) and was incubated for 24 h. Following the incubation, 20 µL of MTT solution (5 mg/mL) was added

in each well and was incubated for 3 h. The media was aspirated and 100 µL of dimethylsulfoxide was accurately pipetted into each well to dissolve the formed formazan crystals. The optical density in each well was observed using ELISA microplate reader (M/s BioTek, Vermont, USA) at 550 nm. Thus, based on the optical density observed, % cell viability was calculated (Eq. 2)[31].

$$\%\text{Cell viability} = \frac{O.D_{\text{treatment}} - O.D_{\text{blank}}}{O.D_{\text{control}} - O.D_{\text{blank}}} \times 100 \quad (2)$$

$O.D_{\text{treatmen}}$t, $O.D_{\text{blank}}$, and $O.D_{\text{control}}$ are the optical densities observed for the treatment, blank (without cells), and the control (without treatment) group, respectively.

Incorporating a diverse array of methodologies, these characterization efforts contributed to a profound understanding of the structural, functional, and biocompatible attributes of liposomal formulations. Each subheading delved into specific facets of the formulations, offering valuable insights that collectively contribute to a holistic comprehension of their performance and potential applications.

Results

In silico analysis

A total of 29 protein structures were predicted using computational modeling tools, including MODELLER 10.2, I-Tasser, and SwissModel. Among these models, the SwissModel-generated model.4 exhibited superior accuracy, as evidenced in Fig. 1, thereby warranting its selection for subsequent docking analyses. Docking studies were conducted across five grid configurations to investigate the binding cavity of the P2X7 receptor, which was homology-modeled using SwissModel. The results are depicted in Fig. 1C, highlighting specific interactions, such as two hydrogen bonds and two Pi-Pi stacking interactions, depicted in distinct colors in Fig. 2. The ligand, Brilliant Blue G dye (BBG250), demonstrated binding interactions with amino acid residues Glu66, Phe97, Tyr111, and Pro112. The XP docking score for this interaction was determined to be − 9.597, An estimated high binding affinity between the ligand (in this case, Brilliant Blue G dye or BBG250) and the P2X7 receptor is indicated by a docking score value of − 9.597. The arbitrary negative sign simply denotes that a lower energy state is connected to a more stable complex. A result of − 9.597 means that there is a strong and favorable binding interaction between BBG250 and the P2X7 receptor, indicating that there is a high probability of the ligand binding to the receptor and creating a stable complex. In comparison, the reference drug, docetaxel, exhibited a docking score of -4.921, indicating lower affinity than BBG250. The observed interactions between BBG250 and the P2X7 receptor, as outlined in Table 6, play a pivotal role in its inhibitory activity. These findings underscore the potential of BBG250 as a candidate for modulating the P2X7 receptor.

Table 6 Amino Acid residues interaction with BBG-250

Ligand	Protein	DOCK Score	H-bond	Pi-Pi stacking	Salt bridge
BBG 250	P2X7	− 9.597	2	2	0

Table 7 Validation of docking result

Ligand	Protein	DOCK Score
Reference compounds		
Docetaxel	P2X7	− 4.921
Positive control (Non-inhibitors)		
ATP (Adenosine triphosphate)	P2X7	− 6.476
BzATP (2′,3′-O-(4-benzoylbenzoyl) adenosine 5′-triphosphate)	P2X7	− 5.494
Negative control (Inhibitors)		
A-438079	P2X7	− 4.499
AZ11645373	P2X7	− 5.595
KN-62	P2X7	− 4.957

The results of the *In silico* ADME study are shown in Tables 7, 8, 9, 10, 11 The physicochemical properties of BBG-250 are reported in Table 7, indicating that BBG-250 possesses molecular weight > 500, several hydrogen bond acceptors between 7, several hydrogen bond donors between 1, several rotatable bonds between 15, and a molar refractivity is 233.61. The lipophilicity profile of selected compounds is reported in Table 8, which suggested that BBG-250 possesses reasonable lipophilic character BBG-250 did not cross the blood–brain barrier. To check the druglikeness parameter, Lipinski & Ghose filter is applied. BBG-250 violet the two Lipinski rule and four Ghose rules (Tables 11, 12, 13). It was observed from the above study that BBG-250 has high GI absorption (Table 10), does not cross the blood–brain barrier, has water solubility (Table 9), considerable lipophilic profile and moderate synthetic accessibility. BBG-250 did not follow the Lipinski rule because of its higher molecular weight (> 500). The accessibility of the compound (BBG-250) was similar to that of the reference drug, docetaxel.

Solubility class: Log S scale. Insoluble < − 10 < Poorly < − 6 < Moderately < − 4 < Soluble < − 2 Very < 0 < Highly.

Lipinski (Pfizer) filter: MW ≤ 500, MLOGP ≤ 4.15, N or O ≤ 10, NH or OH ≤ 5; Ghose filter: 160 ≤ MW ≤ 480, -0.4 ≤ WLOGP ≤ 5.6, 40 ≤ MR ≤ 130, 20 ≤ atoms ≤ 70; Leadlikeness: 250 ≤ MW ≤ 350, XLOGP ≤ 3.5, Number

Table 8 Generated refine model

Model	GDT-HA	RMSD	MolProbity	Varify3D	Errat score	Clash score	Poor rotamers	Rama favored
Initial	1.0000	0.000	1.187	54.56%	90.7955	2.0	1.1	96.8
MODEL 1	0.9705	0.363	1.560	59.55%	93.5943	11.1	0.0	98.1
MODEL 2	0.9753	0.357	1.532	53.82%	88.5714	10.3	0.4	98.4
MODEL 3	0.9769	0.344	1.567	52.87%	88.172	11.2	0.4	98.1
MODEL 4	**0.9697**	**0.363**	**1.574**	**61.78%**	**88.1533**	**11.4**	**0.4**	**98.7**
MODEL 5	0.9721	0.378	1.532	58.60%	87.8571	10.3	0.4	98.4

Bold value indicates the best model

Table 9 Results of ADME study (Physicochemical properties)

S.No	Name	Formula	Mol. Wt. (g/mol)	No. rot bonds	No. H-bond acceptor	No. H-bond donors	Molar refrac-tivity
1	BBG-250	C47H48N3NaO7S2	854.02	15	7	1	233.61
2	Docetaxel	$C_{43}H_{53}NO_{14}$	807.9	14	14	5	205.25

Table 10 Lipophilicity profile of BBG-250

Sl No	Compound name	Log Po/w (XLOGP3)	Log Po/w (WLOGP)	Log Po/w (MLOGP)
1	BBG-250	8.21	10.82	5.67
2	Docetaxel	2.81	2.94	1.06

of rotatable bonds ≤ 7; Synthetic accessibility: from 1 (very easy) to 10 (very difficult).

FTIR spectrum

The FTIR spectrum of HSPC liposomes (P11) revealed characteristic peaks corresponding to various functional groups present in the formulation. Notably, the presence of strong absorption bands around 2920 cm^{-1} and 2850 cm^{-1} indicated the presence of CH stretching vibrations, typically found in lipid chains. The absorption bands around 1736 cm^{-1} indicated the presence of carbonyl (C=O) stretching vibrations, further confirming the presence of lipid components. Additionally, absorption peaks around 1230 cm^{-1} and 1100 cm^{-1} indicated the presence of phosphodiester groups in the formulation, which is consistent with the presence of phospholipids in liposomal formulations (Fig. 3a).

The FTIR spectrum of the pH-sensitive formulation (P5) exhibited distinct peaks corresponding to the specific functional groups present in the formulation. Notably, the absorption bands around 1736 cm^{-1} indicated the presence of carbonyl (C=O) stretching vibrations,

Table 11 Water solubility profile of BBG-250

S No	Compound name	Log S (ESOL)	Solubility (mg/ml)	Class
1	BBG-250	−9.69	1.75e−07	Poorly soluble
2	Docetaxel	−5.85	1.15e−03	Moderately soluble

Table 12 Pharmacokinetics results

Sl No	Compound name	GI absorpti- on	BBB perme -ant	CYP1 A2 inhibit -or	CYP2 C19 inhibit- or	CYP2 C9 inhibit -or	CYP2 D6 inhibi t-or	CYP3 A4 inhibi t-or
1	BBG-250	Low	No	No	No	No	No	No
2	Docetaxel	Low	No	No	No	No	No	Yes

Table 13 Results of druglikeness, leadlikeness

Sl No	Compound name	Druglikeness			Leadlikeness ; violation
		Lipinski rule; Violation	Ghose rule; violation	Bioavailability score	
1	BBG-250	2	4	0.17	3.5
2	Docetaxel	2	3	0.17	2

characteristic of lipid components. The absorption bands around 1650 cm^{-1} indicated the presence of amide I bond, suggesting the incorporation of protein-like components, such as DSPE-PEG_{2000}, within the formulation. Furthermore, absorption peaks around 1100 cm^{-1} and 1050 cm^{-1} indicated the presence of P=O stretching vibrations, confirming the presence of phospholipids (Fig. 3b).

The FTIR spectrum of Brilliant Blue G-250 (BBG-250) showed distinct absorption bands characteristic of the dye molecule. Notably, the absorption peak around 1600 cm^{-1} indicated the presence of aromatic C=C stretching vibrations, confirming the aromatic nature of the dye. The absorption bands around 1300 cm^{-1} and 1200 cm^{-1} indicated the presence of aromatic C-N stretching vibrations, further confirming the structure of the dye (Fig. 3c).

FTIR analysis provided valuable insights into the molecular composition and interactions within the HSPC liposomes, pH-sensitive formulation, and Brilliant Blue G-250 dye. The characteristic peaks observed in the spectra confirmed the presence of specific functional groups and molecular vibrations, further supporting the formulation and characterization of the liposomal delivery system and the dye.

Vesicle shape, size, size distribution, and zeta potential

The quantitative incorporation of BBG-250 into two distinct liposomal formulations was the focal point of the current study. One formulation comprised hydrogenated soya phosphatidylcholine (HSPC) and cholesterol, while the other featured dioleoylphosphatidylethanlamine (DOPE), DSPE-mPEG, DPPC, and cholesterol. A thin film method was employed to create these liposomes, with specific lipid ratios determining their properties. The HSPC and cholesterol ratio of 7:3 yielded liposomes with a vesicular size of 118 ± 1.2 and a polydispersity index (PDI) of 0.316. Similarly, the DOPE, DPPC, DSPE-PEG_{2000}, and cholesterol ratio of 4:3:3:0.3 resulted in liposomes with a vesicular size of 125 ± 1.6 and PDI of 0.165 (Fig. 3 d, e).

Morphology and structure determination

Transmission electron microscopy (TEM) examination revealed the morphology and structural attributes of the formulated HSPC and pH-sensitive liposomes. The TEM images showcased spherical vesicles with uniform size distribution for both formulations. HSPC liposomes exhibited sizes ranging from approximately 100–150 nm, while pH-sensitive liposomes displayed slightly larger sizes spanning 120–180 nm, potentially due to additional components. The lipid bilayer membrane of both liposomal types appeared intact and continuous, affirming their stability and suitability for drug encapsulation and delivery. The TEM results affirmed the successful formation of well-defined liposomal structures, underlining their potential for effective targeted drug delivery applications (Fig. 3f, g).

Analysis of pH levels

The pH values of formulated HSPC (P11) and pH-sensitive liposomes (P5) were measured and found to be 7.3 and 7.8, respectively. These pH values signify the intravenous safety of the liposomal formulations, highlighting their compatibility within physiological pH ranges.

Percentage drug efficiency

The entrapment efficiency of plain dye and HSPC liposome (P11) was determined to be 97% and 70%, respectively. In contrast, the pH-sensitive liposomes (P5) exhibited an entrapment efficiency of 95%. These findings underscore the formulations' capacity to encapsulate the drug effectively.

In vitro drug release studies

The In vitro drug release profiles of both optimized formulations were assessed using a dialysis tube method. The optimized HSPC formulation (P11) displayed a drug release profile of 84.95% over 24 h in PBS 6.4, while the optimized pH-sensitive liposomes (P5) exhibited a drug release of 95% over the same period. These release profiles are visually presented in Fig. 3h, providing a comprehensive depiction of the formulations'-controlled drug release kinetics (Table 14).

Blood compatibility analysis

The blood compatibility of the liposomal formulations was assessed through PT and APTT analyses, evaluating their impact on the extrinsic and intrinsic pathways of blood coagulation. The PT and APTT times for the optimized pH-sensitive formulation (P5) were 12 s and

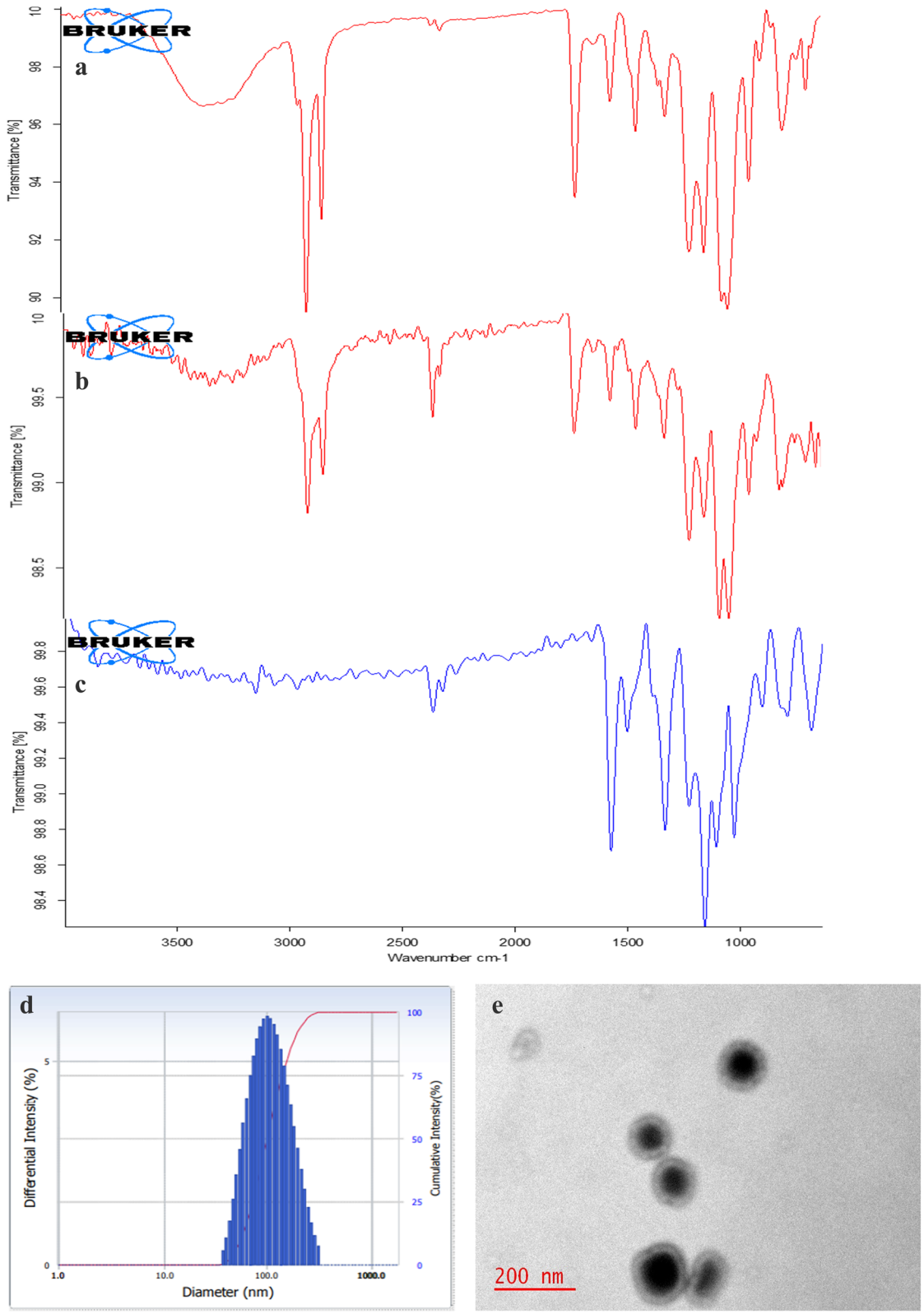

Fig. 3 **a** FTIR spectrum of HSPC liposomes (P11); **b** FTIR spectrum of pH-sensitive formulation (P5); **c** FTIR spectrum of Brilliant Blue G-250 (BBG-250); **d** Particle size of formulation (P5) 118 nm; **e** Zeta potential of formulation (P5) – 25 mV; **f** Microscopic image of formulation (P5); **g** TEM image of formulation (P5); **h** In vitro drug release of formulation pH-sensitive (P5) and HSPC liposomes (P11) in phosphate buffer (pH 6.4); **i** Graph between % viability and concentration of formulation pH-sensitive (P5) and HSPC liposomes (P11), free dye, Docetaxel (DTX)

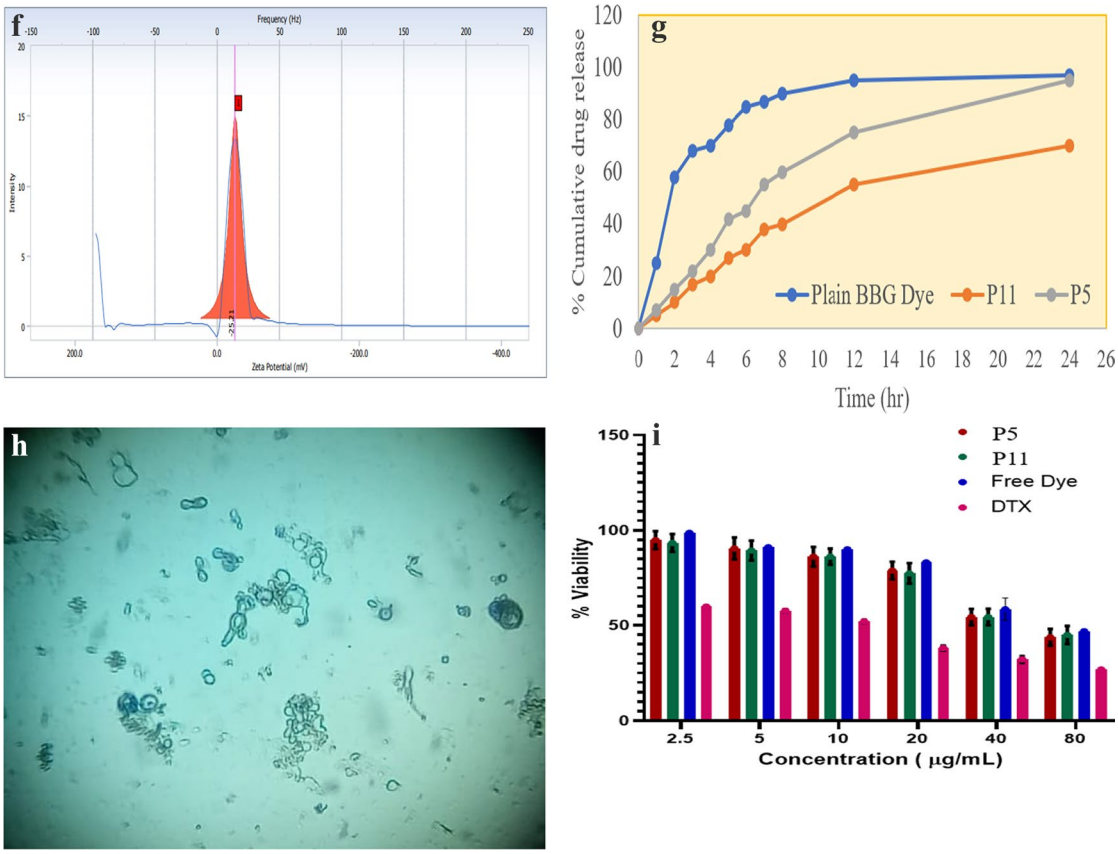

Fig. 3 continued

Table 14 Optimized formulation of conventional and pH-sensitive formulation

Formulation code	Lipid ratio	Drug (mg)	Sonication time	Particle size (nm)	PDI	Entrapment efficiency	Zeta potential
P1	3:2:3:0.3	4	4 min	325 ± 1.6	0.230	49%	−53
P2	3:3:3:0.3	4	4 min	370 ± 0.2	0.165	52%	−55
P3	3:4:3:0.3	4	4 min	390 ± 1.3	0.599	75%	−37
P4	4:2:3:0.3	4	4 min	156 ± 1.4	0.230	72%	−20
P5	**4:3:3:0.3**	**4**	**4 min**	**118 ± 1.2**	**0.165**	**78%**	**−25**
P6	4:4:3:0.3	4	4 min	290 ± 0.8	0.599	65%	−47
P7	5:2:3:0.3	4	4 min	328 ± 0.6	0.230	69%	−30
P8	5:3:3:0.3	4	4 min	425 ± 1.2	0.165	70%	−22
P9	5:4:3:0.3	4	4 min	609 ± 0.6	0.599	45%	−41
P10	8:2:0.3	4	4 min	425 ± 0.6	0.215	**35**	−59
P11	**7:3:0.3**	**4**	**4 min**	**125 ± 0.3**	**0.316**	**64**	**−28**
P12	6:4:0.3	4	4 min	356 ± 0.9	0.366	**52**	−38

Lipid Ratio P1-P9 (DPPC: DOPE: Cholesterol: DSPE-PEG_{2000}); P10-P12 (HSPC: Cholesterol: DSPE-PEG_{2000})

Bold letters highlight the highest drug release in both formulations, whether HSPC or pH-sensitive

43 s, respectively, while the HSPC liposomal formulation (P11) exhibited 14 s and 46 s, respectively. These times, slightly lower than the pH-sensitive formulation, demonstrated a normal safe margin compared to the negative control (saline). The findings as in Table 15 indicated that the liposomal formulations were not

Table 15 Coagulation assay by prothrombin time (PT) and activated partial thromboplastin time (APTT) assessment

S. No	Formulation	APTT Assay	PT assay
1	Normal patient value	45 s	15 s
2	P5	43 s	12 s
3	P11	46 s	14 s

disrupted the blood coagulation pathways, thus confirming their biosafety.

MTT assay: cell viability assessment

The cytotoxicity of HSPC and pH-sensitive liposomes was assessed through an MTT assay on A549 cell lines. The results revealed that both liposomal formulations exhibited cytocompatibility across all concentrations tested. Notably, the MTT profiles illustrated that HSPC and pH-sensitive liposomes displayed significant toxicity toward A549 cell lines compared to blank media. The calculated IC_{50} values further emphasized the formulation's cytotoxic effects, with pH-sensitive formulation, conventional formulation, free drug, and docetaxel having IC_{50} values of 31.6181, 30.2012, 38.8108, and 4.72867, respectively (Fig. 3i, Table 16).

The comprehensive experimental results elucidated the vesicular attributes, drug incorporation efficiency, drug release behavior, blood compatibility, and cytotoxicity profiles of the developed liposomal formulations. These findings collectively contribute to a comprehensive understanding of the formulation's potential biomedical applications and safety considerations.

Discussion

The binding of BBG-250 to the inter-subunit allosteric pocket of the P2X7 receptor in a noncompetitive manner has been established as a safe approach for human administration. In this study, before doing the formulation study we proved interaction between P2X7 and BBG-250 through Docking Study (Fig. 1), and computational ADME study was observed from the above study (Tables 7, 8, 9, 10, 11, 12) that BBG-250 has high GI absorption, not crosses the blood–brain barrier, having water solubility, considerable lipophilic profile. BBG-250 did not follow the Lipinski rule because of higher molecular weight (> 500), so due to this inference, we aimed to explore the potential of liposomal formulations for delivering BBG-250, focusing on formulation comparison, drug release, blood compatibility, and in vitro cytotoxicity. Our findings shed light on the effectiveness of liposomal encapsulation and its implications for antitumoral activity. Formulation optimization is crucial for successful drug delivery. We compared two liposomal formulations: a conventional one composed of HSPC and cholesterol in a 7:3 ratio, and a pH-sensitive formulation consisting of DPPC, DOPE, DSPE-PEG_{2000}, and cholesterol in a 4:3:3:0.3 ratio, both incorporating BBG-250. Microscopic analysis confirmed the vesicles' spherical morphology and uniform size distribution. Size plays a pivotal role in liposome behavior within biological systems. To ensure effective delivery and prevent undesirable accumulation, liposome size is typically maintained below 200 nm. In our study, the conventional and pH-sensitive formulations exhibited sizes of 118 ± 1.2 nm and 125 ± 0.3 nm, respectively, optimizing their potential for tumor targeting while avoiding lung deposition and macrophage clearance. Zeta potential reflects the stability of liposomal suspensions under physiological conditions. The zeta potentials of the conventional and pH-sensitive formulations were − 25 and − 28 mV, respectively, suggesting adequate stability due to the repulsion between particles. The entrapment efficiency and drug loading of both formulations increased with higher drug-to-lipid ratios, indicative of the formulation's capacity to accommodate BBG-250. This finding supports the feasibility of tailoring drug loading based on therapeutic requirements. In vitro, drug release profiles are critical indicators of formulation performance. pH-sensitive

Table 16 Concentration, viability and IC_{50} of formulation pH-sensitive (P5) and HSPC liposomes (P11), free dye, Docetaxel (DTX)

Conc. (µg/mL)	P5		P11		Free Dye		DTX	
	% viability	SD	% viability	SD	% viability	SD	% viability	SD
2.5	94.88542	4.718652	93.40623	4.654433	98.67076	1.0087	59.71	0.61
5	90.52881	5.725947	89.45039	5.152342	91.2	0.702183	57.6	0.85
10	86.21429	5.132336	86.23587	4.221246	90.0381	1.165957	51.95	0.87
20	79.00585	4.603671	77.53959	5.348681	83.30548	0.741875	38.04	1.27
40	54.26522	4.212066	54.25856	4.32278	58.35145	5.786023	32.16	1.74
80	43.68431	4.356637	44.89444	4.736364	46.88714	0.483777	26.85	0.57
IC_{50} (µg/mL)	31.6181		30.2012		38.8108		4.72867	

and conventional liposomes exhibited superior drug release, reaching 95% and 74.95%, respectively, within 24 h, compared to the plain drug solution. This enhanced drug release kinetics in the pH-sensitive formulation aligns with its potential for controlled and targeted drug delivery.

Blood compatibility is a crucial factor for intravenous administration. Our study demonstrated the safety of both conventional and pH-sensitive liposomal formulations in terms of blood coagulation parameters. This highlights their potential for clinical translation and systemic administration. Cytotoxicity assessment using A549 cell lines revealed the effectiveness of both HSPC and pH-sensitive liposomes at various concentrations. The calculated IC_{50} values of 30.2012 ug/ml and 31.6181 ug/ml for HSPC and pH-sensitive liposomal formulations, respectively, indicate their significant toxicity compared to blank media. Notably, the IC_{50} values were approximately 7–eightfold higher than that of docetaxel, a reference drug. In conclusion, nanoscale liposomal formulations offer promising potential for cancer therapy due to their efficient drug delivery and tumor cell penetration capabilities. Our results indicate that liposomes composed of natural SL can serve as stable, biocompatible carriers for BBG-250 delivery, demonstrating the potential for cancer treatment, albeit with less potency compared to the reference drug, docetaxel. Future research could focus on further enhancing liposomal formulation characteristics to optimize antitumoral activity and clinical translatability.

Conclusion

In conclusion, this study establishes the safe and non-competitively binding nature of BBG-250 to the inter-subunit allosteric pocket of the P2X7 receptor for human administration. Computational ADME analysis revealed favorable pharmacokinetic characteristics for BBG-250, while subsequent exploration into liposomal formulations demonstrated their potential as effective carriers for the compound. Both conventional and pH-sensitive liposomes exhibited promising characteristics, including uniform size distribution, stability, and controlled drug release. Notably, pH-sensitive liposomes demonstrated superior drug release kinetics. These findings underscore the potential of liposomal delivery systems for BBG-250, offering a viable avenue for enhancing cancer therapy. Further refinement of these formulations could lead to optimized treatment strategies in the future.

Abbreviations

BBG-250	Brilliant Blue G-250
HSPC	Hydrogenated soya phosphatidylcholine
DOPE	Dioleoylphosphatidylethanolamine
DSPE-mPEG	1,2-Distearoyl-sn-glycero-3-phosphoethanolamine-N-[methoxy(polyethylene glycol)-2000]
DPPC	Dipalmitoylphosphatidylcholine
PBS	Phosphate-buffered solution
PDI	Polydispersity index
TEM	Transmission electron microscopy
PT	Prothrombin time
APTT	Activated partial thromboplastin time
MTT	3-(4,5-Dimethylthiazol-2-yl)-2,5-diphenyltetrazolium bromide
IV	Intravenous
DTX	Docetaxel

Acknowledgements

Authors are thankful to the All India Council for Technical Education (AICTE), New Delhi, India, for financial assistance in the form of PG scholarship to Ms. Twinkle Gupta (ID: 1-9337642145).

Author contributions

All authors, including Twinkle Gupta and Vivek Yadav (formulation and data collection), Sakshi Soni and Sanyog Jain (data collection and interpretation), and Vandana Soni and Sushil Kumar Kashaw (supervisors and manuscript writing), have read and approved the manuscript.

Funding

This work was supported by All India Council for Technical Education (AICTE), New Delhi, with grant number (ID: 1-9337642145).

Availability of data and materials

The data that support the findings of this study are available from the corresponding author, upon reasonable request.

Declarations

Ethics approval and consent to participate

No animal experiments were performed in this work,

Consent for publication

NA.

Competing interests

The authors declare that they have no competing interests.

Author details

[1]Department of Pharmaceutical Sciences, Dr. Harisingh Gour University (A Central University), Sagar, MP 470003, India. [2]Department of Pharmaceutics, Centre for Pharmaceutical Nanotechnology, National Institute of Pharmaceutical Education and Research (NIPER), Sector 67, SAS Nagar (Mohali), Punjab, India.

Received: 29 August 2023 Accepted: 10 January 2024
Published online: 12 February 2024

References

1. Li Z, Feiyue Z, Gaofeng L (2021) Traditional Chinese medicine and lung cancer from theory to practice. Biomed Pharmacother 137:1–5
2. Choi SH, Yoo SS, Lee SY, Park JY (2022) Anti-angiogenesis revisited: reshaping the treatment landscape of advanced non-small cell lung cancer. Arch Pharmacal Res 45(4):263–279
3. Rodak O, Peris-Díaz MD, Olbromski M, Okołów M, Dzięgiel, (2021) Current landscape of non-small cell lung cancer: epidemiology, histological classification, targeted therapies, and immunotherapy. Cancers 13(18):1–33
4. Burnstock G (2008) Purinergic signalling and disorders of the central nervous system. Nat Rev Drug Discov 7(7):575–590
5. Solini A, Chiozzi P, Morelli A, Passaro A, Fellin R, Virgilio F (2003) Defective P2Y purinergic receptor function: a possible novel mechanism for impaired glucose transport. J Cell Physiol 197(3):435–444
6. Di Virgilio F (2012) Purines, purinergic receptors, and cancer. Can Res 72(21):5441–5447

7. Saravanakumar K, Hu X, Vijayakumar S, Wang M (2020) Statistical optimization to augment the photocatalytic reduction of brilliant blue G-250 using the biogenic semiconductor nanorods: an ecosafety approach. J Cluster Sci 31:709–718
8. Sun T, Zhang Y, Pang B, Hyun D, Yang M, Xia Y (2014) Engineered nanoparticles for drug delivery in cancer therapy. Angew Chem Int Ed 53(46):12320–12364
9. Al-Jamal W, Kostarelos K (2011) Liposomes: from a clinically established drug delivery system to a nanoparticle platform for theranostic nanomedicine. Acc Chem Res 44(10):1094–1104
10. Zhong X, Zhu F, Qiao J, Zhao K, Zhu S, Zeng L, Chen X, Xu K (2016) The impact of P2X7 receptor antagonist, brilliant blue G on graft-versus-host disease in mice after allogeneic hematopoietic stem cell transplantation. Cell Immunol 310:71–77
11. Cuthbertson, Peter Mark (2022) The P2X7 receptor in inflammation and disease, doctor of philosophy thesis, school of chemistry and molecular bioscience, University of Wollongong, https://ro.uow.edu.au/theses1/1404, Accessed 22 Dec 2022
12. Young C, Brutkowski W, Lien C, Arkle S, Lochmüller H, Zabłocki K, Górecki D (2012) P2X7 purinoceptor alterations in dystrophic mdx mouse muscles: relationship to pathology and potential target for treatment. J Cell Mol Med 16(5):1026–1037
13. Shen M, Sali A (2006) Statistical potential for assessment and prediction of protein structures. Protein Sci 15(11):2507–2524
14. Arnold K, Bordoli L, Kopp J, Schwede T (2006) The SWISS-MODEL workspace: a web-based environment for protein structure homology modelling. Bioinformatics 22(2):195–201
15. Yang J, Zhang Y (2015) I-TASSER server: new development for protein structure and function predictions. Nucl Acids Res 43(W1):W174-181. https://doi.org/10.1093/nar/gkv342
16. Yang J, Zhang Y (2015) Protein structure and function prediction using I-TASSER. Curr Protoc Bioinform 52(1):5–8
17. Asati V, Bharti S, Das R, Kashaw V, Kashaw S (2022) Discovery of novel ALK2 inhibitors of pyrazolo-pyrimidines: a computational study. J Biomol Struct Dyn 40(20):10422–10436
18. Bhattacharya S, Asati V, Mishra M, Das R, Kashaw V, Kashaw S (2021) Integrated computational approach on sodium-glucose co-transporter 2 (SGLT2) Inhibitors for the development of novel antidiabetic agents. J Mol Struct 1227(129511):1–51
19. Xing X, Ma W, Zhao X, Wang J, Yao L, Jiang X, Wu Z (2018) Interaction between surface charge-modified gold nanoparticles and phospholipid membranes. Langmuir 34(42):12583–12589
20. Kosmerl L (2019) Investigation of bioactive milk phospholipid liposomes and soy phospholipid liposomes on adipocyte physiology. OhioLINK electronic theses and dissertations center http://rave.ohiolink.edu/etdc/view?acc_num=osu1565776533223238 Accessed 22 Dec 2023
21. Huang M, Horwitz TS, Zweiben C, Singh SK (2011) Impact of extractables/leachables from filters on stability of protein formulations. J Pharm Sci 100(11):4617–4630
22. Zangabad PS, Mirkiani S, Shahsavari S, Masoudi B, Masroor M, Hamed H, Jafari Z, Taghipour YD, Hashemi H, Karimi M, Hamblin M (2018) Stimulus-responsive liposomes as smart nanoplatforms for drug delivery applications. Nanotechnol Rev 7(1):95–122
23. Nallamothu R, Wood GC, Pattillo CB, Scott RC, Kiani MF, Moore BM, Thoma L (2006) A tumor vasculature targeted liposome delivery system for combretastatin A4: design, characterization, and in vitro evaluation. AAPS PharmSciTech 7:E7–E16
24. Walunj M, Doppalapudi S, Bulbake U, Khan W (2020) Preparation, characterization, and in vivo evaluation of cyclosporine cationic liposomes for the treatment of psoriasis. J Liposome Res 30(1):68–79
25. Sabeti B, Noordin M, Mohd S, Hashim R, Dahlan A, Akbari Javar H (2014) Development and characterization of liposomal doxorubicin hydrochloride with palm oil. Biomed Res Int 2014:1–6
26. Baxa U (2018) Imaging of liposomes by transmission electron microscopy. Charact Nanoparticles Intended Drug Deliv. 1682:73–88
27. Nunes S, Fernandes R, Cavalcante C, César I, Leite E, Lopes S, Ferretti A, Rubello D, Townsend D, de Oliveira M, Cardoso V (2019) Influence of PEG coating on the biodistribution and tumor accumulation of pH-sensitive liposomes. Drug Deliv Transl Res 9:123–130
28. Sciolla F, Truzzolillo D, Chauveau E, Trabalzini S, Di Marzio L, Carafa M, Marianecci C, Sarra A, Bordi F, Sennato S (2021) Influence of drug/lipid interaction on the entrapment efficiency of isoniazid in liposomes for antitubercular therapy: a multi-faced investigation. Colloids Surf B 208:112054
29. Guimarães D, Cavaco-Paulo A, Nogueira E (2021) Design of liposomes as drug delivery system for therapeutic applications. Int J Pharm 601:120571
30. Dos Santos RB, Oue H, Banerjee A, Kanekiyo T, Singh J (2018) Dual functionalized liposome-mediated gene delivery across triple co-culture blood brain barrier model and specific in vivo neuronal transfection. J Control Release 286:264–278
31. Gaballu FA, Abbaspour-Ravasjani S, Mansoori B, Yekta R, Hamishehkar H, Mohammadi A, Dehghan G, Shokouhi B, Dehbokri SG, Baradaran B (2019) Comparative of in-vitro evaluation between erlotinib loaded nanostructured lipid carriers and liposomes against A549 lung cancer cell line. Iran J Pharm Res IJPR 18(3):1168–1175

Publisher's Note

Springer Nature remains neutral with regard to jurisdictional claims in published maps and institutional affiliations.